

Scientific paper

Structure and Deformational Behavior of Poly(vinylidene fluoride) Hard Elastic Films

Ivan Dmitriev¹, Vili Bukošek², Viktor Lavrentyev¹, Galina Elyashevich^{1*}¹ Institute of Macromolecular Compounds, Russian Academy of Sciences, 31 Bolshoi pr., Saint-Petersburg 199004, Russia;² University of Ljubljana, Faculty of Natural Sciences and Engineering, Snežniška 5, Ljubljana 1001, Slovenia;

* Corresponding author: E-mail: elya@hq.macro.ru

Received: 02-04-2007

Abstract

Effect of annealing on the structure and mechanical properties of melt extruded PVDF films was studied by X-ray scattering, tensile testing, cycling loading, ultrasonic propagation and dynamic mechanical analysis. It has been found that the annealed films prepared at a melt draw ratio higher than 30 and annealed at the temperature close to the melting point exhibit hard elastic properties. Elastic recovery of the annealed PVDF films was about 60%.

Keywords: Poly(vinylidene fluoride); extrusion; annealing; hard elastic films; lamellar structure.

1. Introduction

Hard elastic materials are characterized by a rather high modulus of elasticity and very high elastic recovery typical of elastomers.^{1,2} These remarkable properties of hard elastic systems are due to their specific lamellar supramolecular organization, which is determined by melt extrusion and subsequent isometric annealing conditions. An array of large parallel (stacked) lamellar crystals with lamellar surfaces aligned perpendicularly to the orientation direction is formed in this process.² However the required supermolecular structure has largely been determined to be a complex function of the temperature of extrusion, stress applied during extrusion, cooling parameters, and polymer characteristics (molecular weight, molecular weight distribution, comonomers, etc.). It is generally accepted that formation of initial structure during the extrusion may be described in term of concept of a Deborah number which is defined as the ratio of the characteristic relaxation time for the molecular system divided by the melt process time. When this number approaches unity the process time frame and molecular relaxation time are comparable and this leads to elastic type behavior of a melt. Under influence of extensional flow molecular orientation along the flow direction is realized. Accordingly a higher state of orientation will be achieved as the Deborah number increases.³

Hard elastic materials are of great interest in science and technology due to their unusual mechanical proper-

ties. The deformation mechanism of hard elastic polymers differs from the mechanism of cold drawing of conventional semicrystalline polymer systems which are deformed through neck propagation. This leads to transformation of a lamellar (or spherulitic) structure into a fibrillar one and eventual strengthening of the initial material.^{4,5} No neck develops during the deformation of hard elastics under typical conditions. Deformation of these systems gives rise to bending and moving apart of individual lamellae connected by small amount of statistically distributed bridges of tie chains resulting in the appearance of discontinuities (pores) in the interlamellar space between tie points (Figure 1). Elasticity of a hard elastic material is of the energetic nature because its deformational mechanism consists in lamellae bending in contrast to the entropic deformation mechanism of typical rubbers and semicrystalline polymers. No doubt, the orientation, both on the molecu-

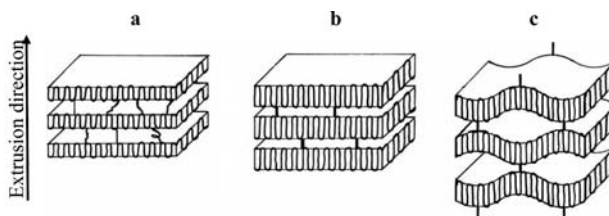


Figure 1. Scheme of the sample structure formed at extrusion (a), annealing (b) and uniaxial extension (c) stages of process.²

lar and supramolecular scale, together with the parameters of a crystalline structure (lamellar thickness, number of tie chains, and distribution of tie chain lengths) are very important factors in providing hard elasticity.

When a hard elastic material is extended to high ratios, the number and sizes of pores between lamellae increase, and the pores become interconnected. Deformation of lamellae and appearance of voids in semicrystalline polymers initiate the formation of microporous systems in the process based on the extrusion-annealing-extension. To the present, the process of microporous materials manufacturing exploiting hard elastic properties of polymers has been elaborated for polyethylene,⁶ poly(propylene),⁷ polyoxymethylene and poly-(4-methyl-1-pentene).^{8,9}

Poly(vinylidene fluoride) (PVDF) is noted for its useful combination of processability, mechanical properties, chemical resistance and also piezoelectric behavior. PVDF is polymorphic polymer: its crystals may be formed in α -, β -, γ -, and α_p -modifications. It is known that uniaxial extension of extruded PVDF films causes piezoelectric β -phase appearance.¹⁰ This ensured that extended PVDF films look very promising for the application in electromechanical devices as a transducer. It has been shown that the formation of a microvoided structure in PVDF results in higher piezoelectric characteristics. A PVDF film is an ideal matrix for preparing composite materials.¹⁰ Moreover, PVDF is a good material for membrane separation. Thus, the investigation of hard elasticity in PVDF films seems to be very perspective.

Investigations of the crystallization behavior of PVDF have shown that melt extrusion can lead to the appearance of “shish” or fiber-like crystals oriented in extrusion direction, which hinder formation of the hard elastic state.^{3,11} It was concluded that PVDF is able of forming the morphology that potentially can ensure hard elastic properties. However, in order to get arguments to success for hard elastic structure formation the mechanical properties of annealed PVDF films should be studied.

This paper is focused on the investigation of the deformational behavior and dynamic properties of annealed PVDF films aimed at the evaluation of the possibility to prepare the hard elastic material. The results will be used for developing of microporous PVDF films preparation process in future studies.

2. Experimental

2.1. Preparation of PVDF Films

Flat PVDF films were formed by melt extrusion (Laboratory extruder “Scamia”, France) using grades of linear PVDF with $M_w = 190000$ and melting point 171 °C. Extruded films (30–60 μm thick) were produced at melt draw ratios λ varying from 8 to 55 and at the melt temperature of 205 °C. The extruded films were annealed with fixed ends at different temperatures during 1.5 hours.

2.2. Mechanical Testing

Stress-strain tests were performed at 20 °C and 100%/min deformation rate on a P-5 tensile test machine (“Tochpribor”, Ivanovo, Russia). Test specimens were cut to 10 mm \times 75 mm stripes with a gauge length of 50 mm (parallel to the extrusion direction).

Hard elasticity was characterized by elastic recovery ϵ_R and work recovery A_R/A_D (see below). These values were determined under five loading – unloading cycles.

2.3. X-ray Diffraction Measurements

The Hermans-Weidinger method was used to determine the degree of crystallinity. Wide-angle X-ray scattering (WAXS) curves were obtained by the DRON-2.0 diffractometer (“Burevestnik”, Saint-Petersburg, Russia) with CuK radiation. According to the calculations of intensities of the meridional X-ray reflections, the crystalline phase of extruded and annealed samples consists of the α -modification alone. (Deformation of hard elastic samples gives rise to polymorphous α – β -transformations but this subject is beyond the scope of this paper.)

Small-angle X-ray scattering (SAXS) curves were measured using reconstructed Kratky camera (A. Paar, Austria) with position sensitive detector. After background subtraction, the collimation and Lorentz corrections were made. Peak positions were employed to obtain long periods according to Bragg’s law.

2.4. Sound Propagation

The sound propagation method was used to characterize the orientation of the samples. Sonic velocity was measured with a PPM-R5 Pulse Propagation Meter (H.M. Morgan, Inc., USA), which produced sound pulses at a frequency of 10 kHz 160 times per second. The apparatus measures electronically the time required for a longitudinal sonic wave to pass through the film between the transmitting and receiving transducers; the sound velocity is then given by the ratio of the distance between transducers to the pulse transit time. The tested samples were fixed with their shorter sides in a frame without any stress. The film was then rotated in its plane, and the angle between the sound propagation and extrusion directions was varied from 0° (extrusion direction) to 90° (cross direction) in 10° increments. The measurements were repeated at least 5 times along each line. The data on sound velocity are presented as polar diagrams.

2.5. Dynamic Mechanical Analysis

A Q800 DMA analyzer (TA Instruments, Delaware, USA) was used in a tension mode. The analyzer was set up with thin film clamps and the Gas Cooling Accessory was used for cooling. The samples were cut to 5-mm wide strips parallel to the extrusion direction. They were fixed

into film clamps and their initial length was set to 10 mm. The clamps were tightened to a torque of approximately 0.14 bars. The measurements were carried out at a frequency of 1 Hz in the temperature range from $-100\text{ }^{\circ}\text{C}$ to $180\text{ }^{\circ}\text{C}$ at a heating rate of $5\text{ }^{\circ}\text{C}/\text{min}$. The deformation strain amplitude was $20\text{ }\mu\text{m}$. To guarantee that the deformation strain is within the linear viscoelastic region of a sample the maximum strain of 0.1% was used.

2. 6. Scanning Electron Microscopy

The surface morphology of PVDF samples was examined by a Scanning Electron Microscopy (JEOL JSM-6060LV). The surface of the film was coated with gold prior to measurements.

3. Results and Discussion

3. 1. Deformational Behavior of the Annealed PVDF Film

The effect of cycling loading on the annealed PVDF film is shown in Figure 2. The film was drawn to 100% extension and then the process was stopped. After five-minute relaxation of the sample the extension-relaxation cycles were repeated five times. According to the basic structural model¹, the deformational behavior of hard elastics may be described by three distinctive regions on the stress-strain curve (Figure 2).

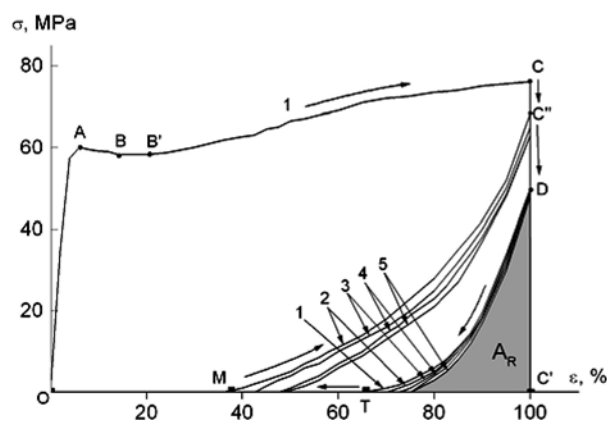


Figure 2. Stress-strain curves at cycling extension of hard elastic PVDF sample ($\lambda = 55$, $T_{\text{ann}} = 170\text{ }^{\circ}\text{C}$). The numbers indicate the strain cycles.

The initial linear part of the curve OA describes the elastic deformation of the sample up to the yield stress point. The elastic modulus of this part of the curve is dominated by the amorphous regions where tie chains bear the main load.

In the second part of the curve, after a short intermediate process (region ABB'), a linear increase in the stress

is observed. This increase is responsible for the elastic character of the lamellar deformation¹, i.e., the energetic origin of hard elasticity. However, the extension of a real lamellar structure with a random distribution of stretched tie chains gives rise not only to the elastic lamellar deformation, but also to some irreversible processes that change the slope of the stress-strain curve. These irreversible processes involve the breakdown of the weakest tie chains, pulling of some network fragments with respect to each other and structural changes of the entire lamellar network. Hence, at the second stage of extension, two deformation modes are involved: elastic recovery of the lamellar network and irreversible deformation accompanied by changes of the lamellar network as a whole. These processes, together with the relaxation of chains in amorphous regions, contribute to the stress at this stage of extension of hard elastic samples.

The transition from the first part of the extension curve to the second one is preceded by a certain decrease in the stress, which is observed when the yield point is attained (AB in Figure 2). This transition corresponds to the change from the uniform elastic deformation mode to another one, which involves both elastic and plastic components.

Once the extension is stopped (point C, Figure 2), irreversible processes (which can be regarded as a viscous flow) cease and their contribution to the deformation stress vanishes. The stress almost immediately drops to the value corresponding to the elasticity of the lamellar network (point D, Figure 2). During the recovery process, when the distance between the fixed ends of the test sample decreases at a constant strain recovery rate, the stored elastic energy of lamellar bending is released, and the stress still goes down. The magnitude of elastic recovery ϵ_R which is equal to MC'/OC' appears to be rather high for PVDF films under study and reaches 60% of the total tensile strain. It should be noted that this value for the samples of flexible chain polymers is usually no more than 5–10%. Work recovery (the portion of the work recovery in the full work at extension) A_R/A_D (ratio of areas $DC'T/MC''C'$ in the cycles following the first one) reaches 40%.

Note that each subsequent curve of cyclic loading lies somewhat below the preceding cycle curve (Figure 2). This implies that the stressed links between lamellae gradually disrupt, and this disruption is the thermofluctuation process.¹² Kinetic thermofluctuation conception established the connection between disruption and thermal fluctuations. At cyclic loading the disruptions are summarized, and the effect of self-heating and structure changes at increasing of number of cycles also start to reveal. The presence of a pronounced yield point is the evidence of a relatively large plastic constituent, which is the main reason for the deviation from a typical stress-strain curve for hard elastic materials. Structurally, it can be explained with an insufficiently high orientation degree. It is shown

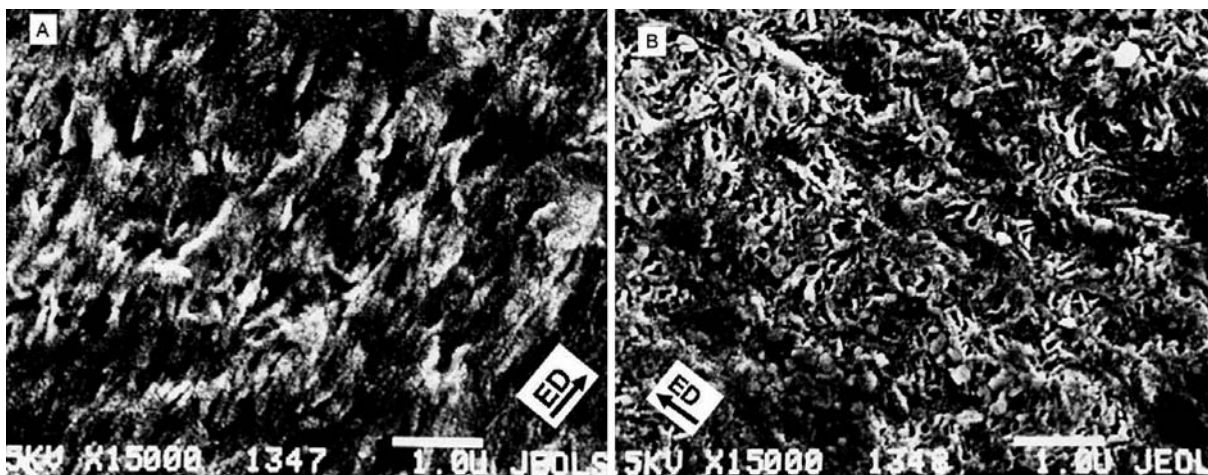


Figure 3. Electron microscopy of surface of PVDF extruded (A) and annealed and extended to 100% (B). Arrows show the extrusion direction.

that the elastic recovery of annealed PVDF fibers with very high $\lambda = 130$ can reach 90%.¹³

There are different approaches to description of hard elastics' deformational behavior.¹³ However, the structural model, which is in good agreement with the results of the polyethylene films investigations,¹⁴ was chosen here. According to this model the deformation mechanism of annealed PVDF films can be characterized as hard elastic behavior. The results of scanning electron microscope investigations of films surface show that surface of the extended hard elastic samples contains the pores in contrast to of the initial samples morphology (Figure 3). The influence of melt draw ratio and annealing temperature on the properties of PVDF hard elastics will be discussed below.

3. 2. Effect of Melt Draw Ratio and Annealing Temperature on Mechanical Properties of Hard Elastic Samples

Extruded films were formed at various melt draw ratios (λ). Then these films were annealed under isometric conditions (the ends of the samples were fixed) at 170 °C. Figure 4 shows the stress-strain behavior of extruded and annealed PVDF films. It can be seen from the figure that the ability of extruded samples to deform and develop stress is strongly enhanced with increasing λ . For all samples the growth of crystallinity after annealing is observed (Figure 5); and this effect is more pronounced for the higher λ that confirms the model of structure transformations presented in Figure 1. However, the difference in the mechanical properties for the samples prepared at various λ is preserved. The stress-strain curve of the annealed film formed at $\lambda = 8$ (curve 1') shows a small sample elongation after transition through a strongly pronounced yield point. Obviously, this sample does not exhibit any hard elastic behavior. The deformational behavior of the annealed films prepared of the samples extruded at $\lambda = 30$ (curve 2') displays a lower yield stress and a weak growth of the

stress at the part of the curve following the yield point. This means that the elastic component is not sufficiently large to consider the structure as hard elastic. The deformational behavior of the films prepared at the largest $\lambda = 55$ (curve 3') corresponds most of all to the hard elasticity model. Further, it is seen that the length of the horizontal region following the yield point (necking region, corresponding to the BB' region in Figure 2) decreases for annealed films (curve 3') as compared with extruded ones (curve 3). The fact that annealing leads to the increase in the Young modulus (initial slope of the curves in Figure 4) is the evidence that the plastic component of deformation suffers a loss. Thus, annealing effectively influences on the sample structure by initiating hard elasticity in the films extruded at $\lambda = 55$.

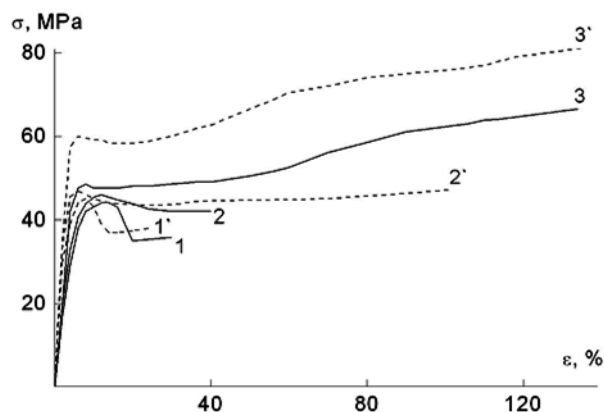


Figure 4. Stress-strain curves for extruded (1, 2, 3) and annealed (1', 2', 3') PVDF samples prepared at $\lambda = 8$ (1, 1'), 30 (2, 2'), 55 (3, 3').

The increasing of intensity of small angle X-ray diffraction was observed after annealing (Figure 6). It is known that intensity of SAXS is proportional to difference between densities of crystalline and amorphous phases. It means that the annealing leads to the decreasing of

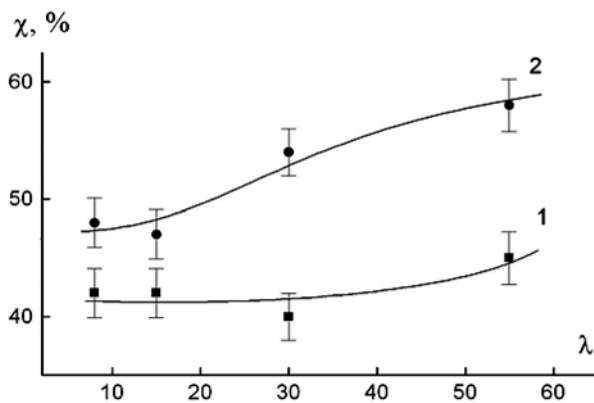


Figure 5. Dependence of X-ray crystallinity on melt draw ratio (λ) for extruded (1) and annealed (2) PVDF films.

density of amorphous zones due to the lowering of the interlamellar tie chains concentration. Calculated values of X-ray long periods inconsiderably depend on λ , but they increase after annealing from 12 to 17 nm.

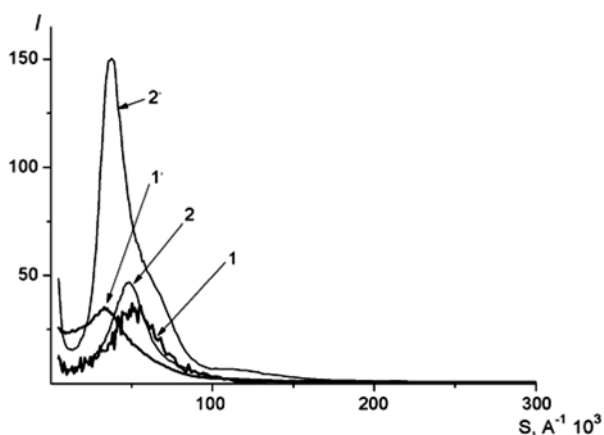


Figure 6. Small-angle X-ray scattering curves for extruded (1, 2) and annealed (1', 2') PVDF samples prepared at $\lambda = 15$ (1, 1') and 55 (2, 2').

Figure 7 demonstrates the influence of annealing temperature on the mechanical properties of the annealed films ($\lambda = 30$). The increase in annealing temperature results in the growth of break elongation and Young modulus (from 1350 to 1900 MPa). The rise of curve 4 (Figure 7) at the strains more than the yield point can be regarded as the indication that hard elasticity is developed. This fact was verified by calculating the elastic recovery and the work recovery which grow considerably with increasing annealing temperature, especially as this temperature approaches the PVDF melting point (Figure 8). Large values of ϵ_R and A_R/A_D presented in Figure 8 for high annealing temperatures are typical of the hard elastic samples obtained from other flexible-chain polymers, such as polypropylene and polyethylene.^{1,2,14}

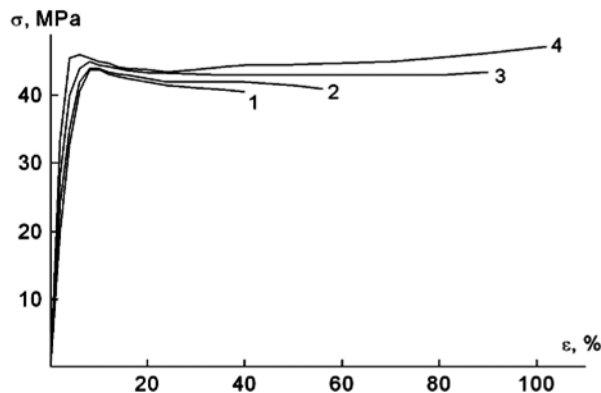


Figure 7. Stress-strain curves for PVDF films: extruded (1) and then annealed at temperatures 100 (2), 140 (3), 170 °C (4). Extruded films were prepared at $\lambda = 30$.

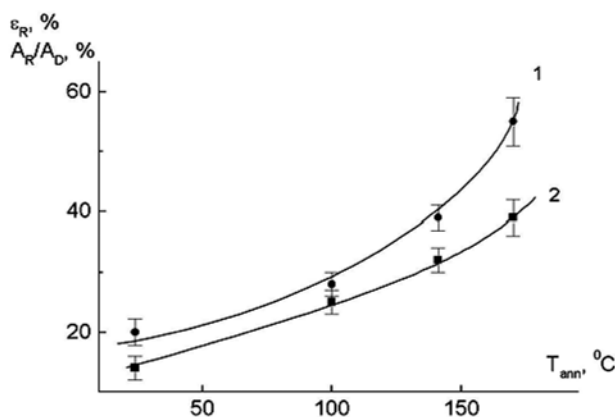


Figure 8. Dependences of elastic recovery (1) and work recovery (2) at deformation of hard elastic PVDF films at $\lambda = 30$ on annealing temperature (in the fifth cycle of loading to 50% extension).

3. 3. Structure Changes Under Annealing Studied by Sound Propagation

In order to characterize the effect of λ on structure transformations at annealing, sonic velocity measurements were performed. Polar diagrams of the sound propagation velocity V and the absolute values V for extruded and annealed films are presented in figure 9 and Table 1. It can be seen (Figure 9) that all extruded samples are characterized by anisotropy of sound velocity V_t/V_0 . This value is larger for the samples prepared at higher λ . The highest magnitudes of V were observed in the transverse direction, which confirms the model of stacked lamellar structure in which flat crystallites are located transversely to the machine direction.² Absolute magnitudes of V for the extruded films with $\lambda = 30$ are lower than for those with $\lambda = 8$ in both directions, but anisotropy is higher for the more oriented samples (Table 1). The observed decrease in sound velocity with increasing λ obviously reflects a lower structural continuity because of higher un-packing in the amorphous matrix or, generally, by a lower number of tie chains connecting crystalline lamellae.¹⁵

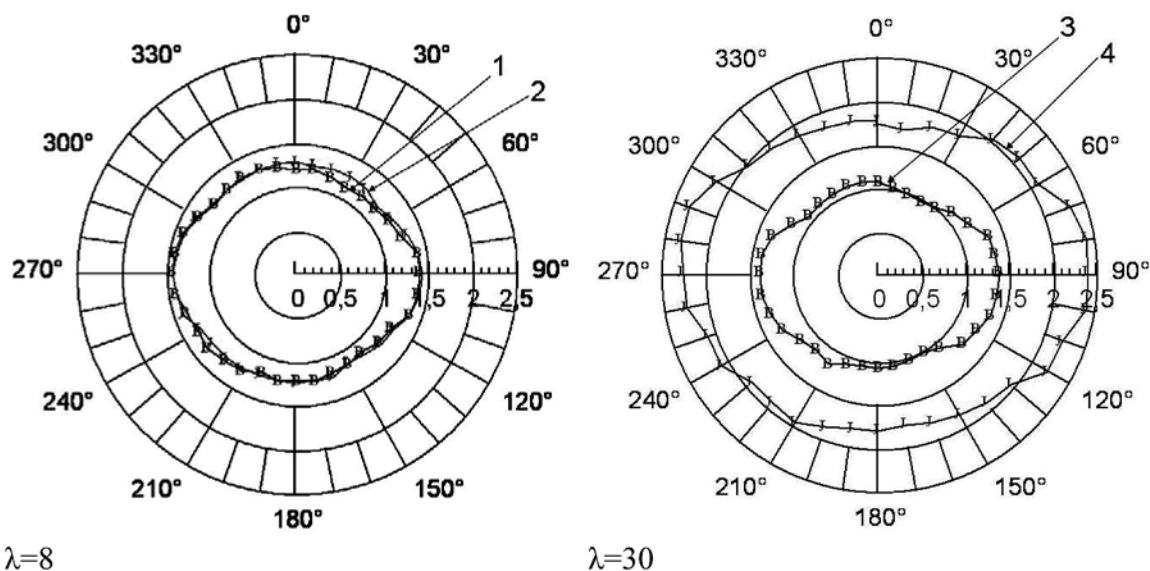


Figure 9. Polar diagrams of sound propagation velocity (km s^{-1}) for extruded (1, 3) and annealed (2, 4) PVDF samples prepared at $\lambda = 8$ (1, 2) and 30 (3, 4). 0–180° – orientation direction.

Table 1. Sound velocity for extruded and annealed PVDF samples. (V_o – orientation direction; V_t – transverse direction)

Sample	Sound velocity, km/s					
	$\lambda = 8$			$\lambda = 30$		
	V_o	V_t	V_t/V_o	V_o	V_t	V_t/V_o
Extruded film	1.212	1.412	1.165	1.085	1.385	1.276
Annealed film	1.225	1.429	1.166	1.782	2.287	1.283

As seen in the Table 1, absolute values and anisotropy of sound velocity for the annealed samples are higher than for the films extruded at all λ , but for the samples prepared at $\lambda = 30$ this effect is more pronounced. Moreover, the absolute values of sound velocity for the annealed samples extruded at $\lambda = 30$ are markedly higher than those for the samples obtained at lower λ (in contrast to the extruded samples). Therefore, the effect of annealing on sound velocity is much stronger for the films obtained at $\lambda = 30$. Similar results were observed for polyethylene hard elastic films.¹⁶ Thus, these data confirm the fact established earlier for polyethylene that a necessary precondition for the appearance of hard elasticity in annealed samples is a high orientation degree of extruded samples.¹⁷

3. 4. DMA Investigations of Extruded and Annealed PVDF Samples

It is known that amorphous chains with different degrees of mobility are responsible for elastic properties of semicrystalline polymers. In order to analyze the structure transformations at isometric annealing, the relaxation investigations of PVDF samples were carried out by dynamic mechanical measurements. In Figure 10, dynamic

mechanical relaxation spectra for the extruded and annealed PVDF film formed at $\lambda = 30$ are presented. Two distinct relaxation peaks for the extruded sample designated as α_a (-40°C) and α_c ($\sim +80^\circ\text{C}$) are seen on curve 1. The α_a -relaxation process in PVDF has been attributed to the cooperative segmental motion.¹⁸ So far, the origin of α_c -relaxation has not been understood sufficiently well, however, many investigators explain it by the mobility in disordered regions in crystallites and intermediate layers between amorphous and crystalline regions. It is believed that α_c -transition is related to the amorphous segments suspended from chain-folded lamellae surfaces and to the tie chains directly linking adjacent lamellae. At the same

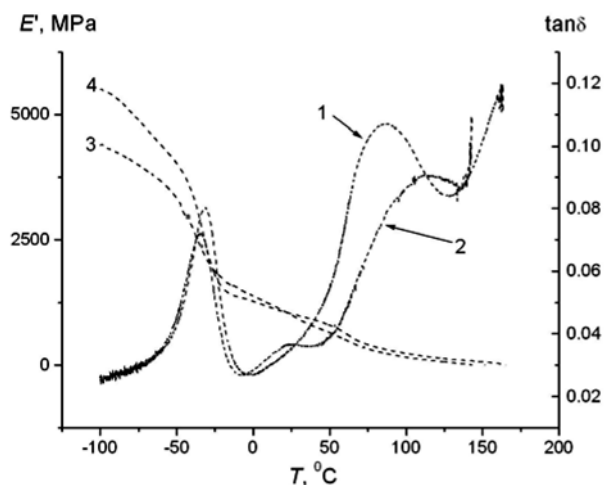


Figure 10. DMA spectra for extruded (1, 3) and annealed (2, 4) PVDF samples prepared at $\lambda = 30$: loss factor $\tan\delta$ (1, 2) and storage modulus E' (3, 4).

time, there is an opinion that α_c -transition is also related to the mobility in crystal regions. According to,¹⁹ the polymers without α_c -transition are not capable of orientation drawing, since chain translations through crystals are not possible at the energies below the chain rupture.

It can be seen (Figure 10) that there are three regions on the temperature dependence of Young modulus in the range between α_a - and α_c -transitions (curve 3). Three mechanisms of PVDF deformation correspond to these regions. At temperatures below the glass transition, Young modulus reaches maximal values due to the whole amorphous phase being glassy. In the temperature range between the α_a - and α_c -processes, the amorphous phase is liquid-like, but certain constrained amorphous regions and/or defects inside crystallites have no mobility. Above the temperature corresponding to the α_c -process, the mobility of the amorphous phase as a whole increases that leads to decreasing Young modulus.

The amorphous-crystalline interphase in semicrystalline polymers possessing α_c -relaxation affects elastic properties of these polymers at room temperature, and they can be controlled by a preliminary thermomechanical treatment.²⁰ Figure 10 shows that annealing at the temperatures close to the melting point (171 °C) does not influence on the position of the glass temperature (α_a -process), but the second transition (α_c -process) shifts to higher temperatures (curve 2). The annealing leads to the perfection and thickening of lamellae due to involving of the interphase chains into the crystals up to full straightening (Figure 1b). A significant increase in crystallinity (Figure 5) confirms that lamellae growth takes place. As a result of this process and fixation in crystals at annealing, tie chains become stressed and rigidly connect lamellae. The deformation of this system is realized as a reversible process of lamellae deformation between these “bridges”. Realization of the chains movement in the interphase of such hard structure requires a higher temperature that is demonstrated by the shift of the second maximum (Figure 10).

4. Conclusions

The structure – deformation relation of annealed PVDF films has been studied. It has been shown that annealed films exhibit hard elastic properties. The characteristics of a hard elastic effect in PVDF depend on the initial degree of orientation (melt draw ratio) and annealing temperature of extruded films. It has been established that hard elastic properties appear under the conditions of high orientation in the initial structure. Hard elasticity becomes more pronounced as the annealing temperature increases up to the melting point of PVDF. Annealing of PVDF extruded films results in a higher crystallinity and a shift of the relaxation transition responsible for mobility in the crystalline interphase to higher temperatures because of chain straightening. A

hard elastic system is formed due to the radical transformation in crystalline and amorphous parts. Thus, the behavior of these samples at uniaxial extension is determined by deformation of large and highly oriented lamellar crystallites connected by stressed tie chains. It has been demonstrated that the deformational behavior of these systems is similar to that of hard elastics of polypropylene and polyethylene.^{1,2,6,16}

5. Acknowledgements

The work was supported by the Russian Foundation for Basic Research (Grant № 07-03-00177) and by the Programme for Basic Research, Russian Academy of Sciences, Division of Chemistry and Material Sciences, “Synthesis and Investigations of New Polymer Systems Containing Polyconjugated Polymers and Possessing Semiconducting and Conducting Properties”, direction “Conductive and Electroconductive Polymers” (2006–2008).

The authors also wish to thank Marjeta Radišek from Instrumentalia (Ljubljana) and N. Hawkins from TA Instruments (both University of Ljubljana) for their kind assistance and cooperation.

6. References

1. B. S. Sprague, *J. Macromol. Sci.* **1973**, *8*, 157–187.
2. I. K. Park, H. D. Noether, *Colloid. Polym. Sci.* **1975**, *53*, 824–839.
3. J. Xu, M. Johnson, G. L. Wilkes, *Polymer*. **2004**, *45*, 5327–5340.
4. A. Peterlin, *Polym. Eng. Sci.* **1976**, *16*, 126–137.
5. G. K. Elyashevich, E. A. Karpov, E. Yu. Rosova, B. V. Streltsevs, V. A. Marikhin, L. P. Myasnikova, *Polym. Eng. Sci.* **1993**, *33*, 1341–1351.
6. G. K. Elyashevich, A. G. Kozlov, E. Yu. Rosova, *Polym. Sci. (translated from Russian)*. **1998**, *40A*, 567–573.
7. S. L. Cannon, W. O. Statton, J. W. S. Hearle, *Polym. Eng. Sci.* **1975**, *15*, 633–646.
8. M. B. Johnson, G. L. Wilkes, *J. Appl. Polym. Sci.* **2001**, *81*, 2944–2963.
9. M. B. Johnson, G. L. Wilkes, *J. Appl. Polym. Sci.* **2002**, *83*, 2095–2113.
10. J. C. McGrath, L. Holt, D. M. Jones, I. M. Ward, *Ferroelectrics*. **1983**, *50*, 13–20.
11. J. M. Samon, J. M. Shultz, B. S. Hsiao, S. Seifert, N. Stribeck, I. Gurke, G. Collins, C. Saw, *Macromolecules*. **1999**, *32*, 8121–8132.
12. S. N. Zhurkov, *Internat. J. Fracture Mech.* **1965**, *4*, 311–323.
13. C.-H. Du, B.-K. Zhu, Y.-Y. Xu, *Macromol. Mater. Eng.* **2005**, *290*, 786–791.
14. G. K. Elyashevich, E. A. Karpov, A. G. Kozlov, *Deformation behavior and mechanical properties of hard elastic and po-*

- rous films of polyethylene. In: *Mechanical Behavior of Polymeric Materials* (Ed. Kahovec J.), WILEY-VCH Verlag GmbH, Prague, 1999, 91–101.
15. I. Yu. Dmitriev, S. V. Gladchenko, V. K. Lavrentyev, O. E. Praslova, G. K. Elyashevich, *Russ. J. Appl. Chem. (translated from Russian)*. 2006, 79, 642–646.
16. M. Raab, J. Scudla, A. G. Kozlov, V. K. Lavrentyev, G. K. Elyashevich. *J. Appl. Polym. Sci.* 2001, 80, 214–222.
17. G. K. Elyashevich, A. G. Kozlov, I. T. Moneva, *Polym. Sci. (translated from Russian)*. 1998, 40B, 71.
18. N. K. Kalfoglou, H. L. Williams, *J. Appl. Polym. Sci.* 1973, 17, 3367–3373.
19. E. S. Clark, L. S. Scott, *Polym. Eng. Sci.* 1974, 14, 682–686.
20. B-E. El Mohajir, N. Heymans, *Polymer*. 2001, 42, 5661.

Povzetek

Vpliv tempranja na strukturo in mehanske lastnosti poliviniliden-fluoridnega (PVDF) filma, ekstrudiranega iz taline, smo zasledovali z rentgenskim sipanjem, nateznim poskusom, cikličnim obremenjevanjem, hitrostjo razširjanja zvoka in dinamično mehansko analizo. Ugotovljeno je, da kažejo žilavo-elastične lastnosti filmi pripravljeni s predilnim razteznim razmerjem višjim od 30 in temprani pri temperaturi blizu tališča. Elastična povrnjivost (relaksacija) tempranih PVDF filmov je okoli 60 %. Žilavo-elastične lastnosti so posledica strukturnih in sprememb molekulske gibljivosti pri tempranju.